Delineation of Dry and Melt Snow Zones in Antarctica Using Microwave Remote Sensing Data

Hongxing Liu and Lei Wang
Department of Geography
Texas A&M University
College Station, TX 77843, USA
liu@geog.tamu.edu
wanglei@geog.tamu.edu

Kenneth C. Jezek
Byrd Polar Research Center
The Ohio State University
Columbus, OH 43210, USA
jezek@frosty.mps.ohio-state.edu

Abstract— **This paper presents the analysis results for delineating snow zones in Antarctica using active and passive microwave satellite remote sensing data. With a high-resolution Radarsat SAR image mosaic, we have successfully delineated dry snow zones, percolation zones, wet snow zones, and blue ice patches for the Antarctic continent. With the daily passive microwave SSM/I data, we derived dry and melt snow zones. The analysis results respectively derived from the SSM/I and the Radarsat SAR data were compared and correlated. We demonstrated the complimentary nature and comparative advantages of frequently repeated passive microwave data and spatially detailed radar imagery for detecting and characterizing snow zones.**

Keywords- snow zones, SAR, passive microwave, Antarctica

I. INTRODUCTION

In this paper, we present numerical algorithms and analysis results for delineating snow zones in Antarctica with active Radarsat SAR imagery and passive microwave SSM/I data. Based on radar backscatter characteristics of different snow zones, we developed a numerical method and derived snow zones from SAR imagery. The method consists of a sequence of image processing algorithms. A competing region growing and merging algorithm was used to classify the radar image into a series of homogeneous regions. Based on the radar backscatter characteristics and texture information, the image regions are further classified and labeled into different types of snow zones. The heuristic higher-level knowledge about the areal size and adjacency properties of snow zones were utilized to detect and correct misclassifications induced by SAR image noise, and relief-induced radiometric distortions. With high-resolution Radarsat SAR imagery acquired in 1997, we delineated dry snow zones, percolation zones, wet snow zones and blue ice patches over the entire Antarctic Ice Sheet and surrounding ice shelves. Based on the passive microwave data, we also derived the snow melt onset date, melt end date and melt duration for the period 1991-1997 with a multi-scale wavelet transform based edge detection method [1]. The comparison between the high-resolution snow zone boundaries from the SAR imagery with melt extents derived from time series passive microwave data suggests that the percolation and wet snow zones detected from SAR imagery represent the snow melt extent integrated over many years prior to the SAR image acquisition. By using passive microwave data, we were also able to determine the melt intensity for the wet snow zone, which was delineated from SAR imagery.

II. DELINEATION OF SNOW ZONES USING RADARSAT SAR IMAGERY

A. Ortho-rectified Radarsat SAR image Mosaic for Antarctica

We used the Radarsat-1 Synthetic Aperture Radar (SAR) image mosaic of Antarctica for our analysis (Figure 1). The mosaic was compiled from data acquired by a C-band (5.6 cm wavelength) SAR sensor onboard the Canadian Radarsat-1 satellite. The imaging campaign was conducted from September 9 to October 20, 1997 [2]. The coastal regions were imaged mainly using the standard beam 2 with a nominal incidence angle of 24°-31° at 25 m resolution. This precisely geocoded and terrain corrected image mosaic furnishes a planimetrically accurate radar image base for interpreting and delineating different snow zones at continental scale.

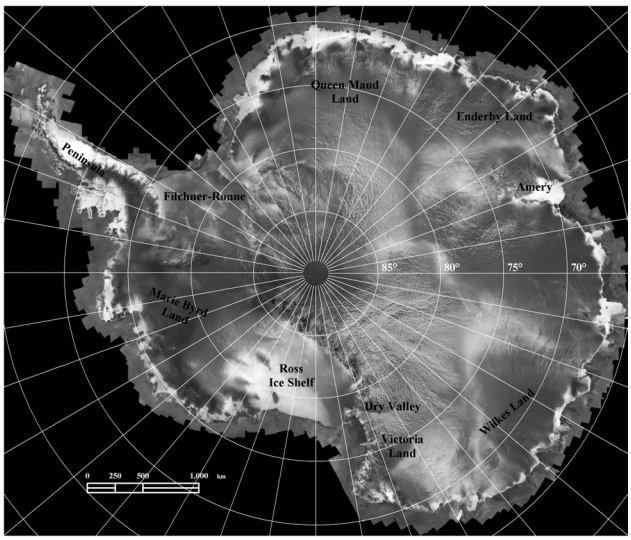

Figure 1: Orthorectified SAR image mosaic for Antarctica, in which source images were acquired in September and October, 1997 by Radarsat-1 C-band SAR sensor.

B. Radar Backscatter Signatures of Different Snow Zones in Antarctica

A close visual examination confirmed that the winter SAR image mosaic has sufficient brightness contrasts for discrimination of different snow zones. The strong contrast in radar backscatter exists between dry snow zones and percolation zones. This makes the discrimination between the dry snow zone and the percolation zone relatively easy and reliable. Differences in the radar backscatter between the percolation zone and the wet snow zone are also evident. The frozen melt ponds can be clearly observed in the wet snow zone. Generally speaking, the superimposed bare ice zone in Benson's model [3] is absent in Antarctica due to its relatively high latitude. Nevertheless, blue ice patches [4] exposed by sublimation and katabatic wind scouring can be observed in both percolation zones and dry snow zones as isolated islands. In general, the radar backscatter strength of blue ice patches is lower than wet snow zones and higher than dry snow zones in the winter SAR imagery. The spatial extents of blue ice patches are relatively small, and their textures are characterized by ripples, cusps and stripes caused by katabatic winds and compressive ice flows.

To derive a quantitative signature for each type of snow zone, we identified a number of training sites respectively for dry snow zones, percolation zones, wet snow zones, and blue ice patches in different parts of Antarctica. Based on the training data sets, the statistical characteristics of radar backscatter are analyzed for each type of snow zones.

C. Automated Algorithms for Snow Zone Extraction

We designed a chain of image processing steps to automate the extraction of snow zone boundaries from the SAR imagery based on the image segmentation. The key processing steps include: image segmentation with a competing region growing and merging algorithm; region labeling and classification based on the backscattering and texture properties; and post-classification processing based on higher-level knowledge about size and adjacency relationships between snow zones.

D. Dry Snow Zones, Percolation Zones, Wet Snow Zones and Blue Ice Patches from SAR imagery

By applying the above sequence of image processing algorithms and parameter settings, the snow zone boundaries are numerically derived for the entire Antarctica with minimal human intervention and editing effort.

The whole sequence of snow zones in Benson's model [3], except for the superimposed bare ice zone, occurs in the Antarctic continent. As shown in Figure 2, the dry snow zones are spatially extensive and continuous. The interior of the ice sheet and the central plateau of the mountain chain in the Antarctic Peninsula are occupied by the dry snow zones. Isolated small dry snow zones are also observed in the top parts of ice rises and islands in the ice shelves due to higher elevations. The majority of the Ronnie and Filtchner Ice Shelf, and the southern and eastern parts of the Ross Ice Shelf are located in the dry snow zone due to their high latitudes. Overall, the dry snow zones dominate the Antarctic continent, accounting for 89.84% of the total area.

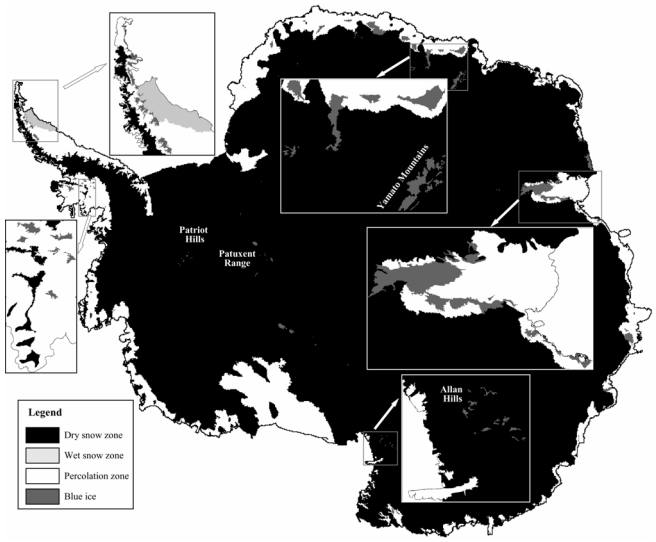

Figure 2: Dry snow zones, percolation zones, wet snow zones, and blue ice patches in Antarctica derived from Radarsat SAR image mosaic.

The percolation zone indicates the extent of snow surface that are at least occasionally affected by melt events. Extensive percolation zones are detected on the ice shelves with relatively low latitude, including the Larsen Ice Shelf, the George IV Ice Shelf, the Amery Ice Shelf, the West Ice Shelf, the ice shelves along Queen Maud Land and Marie Byrd Land, and the western part of the Ross Ice Shelf. The percolation zones on the grounded ice sheet are confined to a narrow band of varying width near the coast (Figure 2).

In Antarctica, the extent of the wet snow zone is spatially insignificant. It is only distributed on the northern part of the Antarctic Peninsula.

The detected blue ice patches are distributed in both percolation zones and dry snow zones where the surface slope is relatively steep. As shown in Figure 2, small blue ice patches are distributed in the percolation zones on the Antarctic Peninsula, in the Amery Ice Shelf region and in Queen Maud Land region. The expanses of blue ice fields are also detected in dry snow zones in the Transantarctic Mountains near Allan hills and Patuxent Range, in the Ellsworth Mountains near Patriot Hills, and in the Yamato (Queen Fabiola) Mountains and Sør Rondane Mountains in Queen Maud Land (Figure 2). Most blue ice fields in the dry snow zones are found in the leeside of mountain ranges and nunataks. It should be pointed out that the blue ice areas are not located at a lower elevation as a continuous zone surrounding the wet snow zone. The blue ice areas form largely because of the upwelling of deep glacial ice on the flanks of the mountains and nunataks, surface snow being blown away by gusty katabatic winds, and the firn subliming away to the atmosphere. In terms of the location, formation, spatial extent and continuity, the isolated blue ice patches cannot be regarded as the superimposed bare ice zone in Benson's model.

III. DELINEATION OF SNOW ZONES USING SSM/I DATA

A. Melt Detection and Mapping Algorithms

Based on the wavelet transform of the daily brightness temperature time series, we developed a multi-scale edge detection method for deriving snow melt onset date, melt end date, melt duration, and melt extent [1]. To obtain the precise timing of melt and freeze occurrences, our method explicitly searches and tracks strong edges on brightness temperature curves induced by melt and refreeze events across scales.

B. Melt Extent and Duration Derived from SSM/I Data

In order to compare and correlate the snow zones detected from the 1997 winter SAR imagery, we processed the satellite passive microwave SSMI data from July 1, 1991 to June 30, 1997 collected by the DMSP- F8, F11, and F13 satellites. The SSM/I data have seven different channels: 22 GHz vertically polarized channel and 19 GHz, 37 GHz and 85 GHz for both horizontally and vertically polarized channels. Our experiments showed that although all channels show similar responses to melt events, the 19 GHz horizontally polarized channel exhibits the strongest melt-induced edges on the Tb time series and hence was selected for our snow melt analysis. This channel has an effective field of view of 70 km along-track and 45 km cross-track. The resampled pixel size for this channel is 25 km, and a grid of 182x222 pixels covers the entire Antarctic continent. A coastline mask [5] is applied to remove ocean pixels. The analysis was only carried out for pixels that lie on the ice sheet and ice shelves in order to eliminate ocean contamination. For each ice pixel, we form 365 days of Tb time series starting with July 1 as the first day in order to center the Antarctic austral summer season in the middle of the Tb curve. The melt onset date, melt end date, and melt duration are computed sequentially for every data pixel. The pixel-by-pixel computation produces three grids each year during 1991-1997: melt onset date grid, melt end date grid, and melt duration grid. The melt duration map (Figure 3) demonstrated the spatial variation of melt intensity across the Antarctic continent.

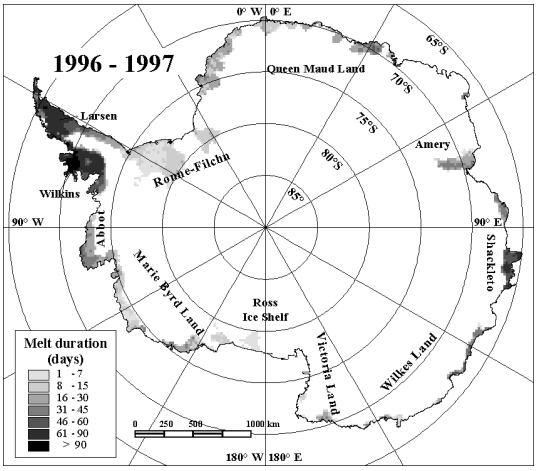

Figure 3: Snow melt duration (cumulative melt days) during 1997-1998.

IV. COMPARISONS AND ANALYSIS

Analysis results derived from both active SAR imagery and passive microwave SSM/I data indicate that Antarctic ice surface melting is sparse and concentrated in the periphery of the Antarctic continent. However, the spatial coverage of the melt snow zones derived from the 1997 winter SAR image mosaic is significantly different from that detected from the SSMI daily brightness temperature data during the 1996/1997 austral summer (Figure 4a). The matching rate between the SAR-derived melt zone extent and the passive microwave derived melt extent for the 1996/1997 summer is only 61%.

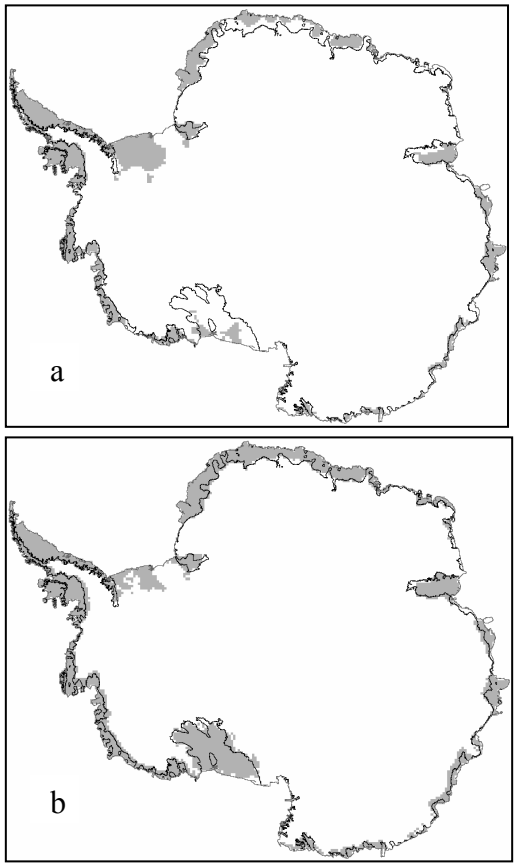

Figure 4: Snow zone boundaries derived from the 1997 SAR image mosaic compared with snow melt extents derived from the passive microwave. (a) The shaded area is the snow melt extent during the 1996/1997 austral summer. (b) The shaded area is comprised of pixels whose average annual melt duration in the past six austral summers from 1991 to1997 is longer than 3 days.

The discrepancies suggest that the melt snow zone from SAR imagery does not represent the melt extent for the year when the SAR imagery was acquired. Notably, no surface melting was observed from the passive SSM/I data in many small ice shelves along the coast of Queen Maud Land. However, the percolation zones were detected in these regions from the 1997 winter SAR imagery. An extensive percolation zone is delineated from the SAR imagery on the Ross Ice Shelf, where only brief melting for two small areas was detected by the passive microwave sensor. In addition, the effect of the short-lived melting in the rim of the Ronne-

Filtchner Ice Shelf in the 1996/1997 austral summer detected from passive microwave SSM/I data does not show up on the 1997 winter SAR imagery. This is likely because the melting is not intensive enough to develop the ice pipes and ice lenses, or because new snowfall after the summer precluded the melting effect from being detected by the SAR sensor. It is known that the Ronne-Filchner Ice Shelf has a much higher snow accumulation rate than the Ross Ice Shelf [6].

As shown in Figure 4b, the averaged snow melt extent during 1991-1997 derived from the passive microwave SSM/I data has a much better correspondence with that derived from the 1997 winter SAR image mosaic. The shaded area in Figure 12b represents the cumulative melt area with averaged annual melt duration of at least 3 days during the austral summers from 1991 to 1997. The matching rate between the snow melt extent derived from the 1997 SAR image and the averaged snow melt extent during 1991-1997 detected by the passive microwave data is 93%. The greatly improved match suggests that the snow melt zone derived from SAR imagery may represent a composite signal of intermittent melt events summed over many years. In areas with low accumulation (less than the radar penetration depth) in intermittent melt years, the radar backscatter signal may still be strong even though the last melt event may have occurred years ago. In the case of the Ross Ice Shelf, a short-period but spatially extensive melting was detected during the 1991/1992 austral summer, and no substantial surface melting was detected afterwards until 1997. The melting effect was still detected by the SAR sensor after 6 years, and hence an extensive percolation zone was delineated. This can be probably attributable to the extremely low snow accumulation on the Ross Ice Shelf.

V. DISCUSSIONS AND CONCLUSIONS

Our analysis shows that both active and passive satellite microwave sensors are useful for the discrimination of the melt snow zone from the dry snow zone. However, it should be emphasized that the melt snow zones derived from active and passive microwave data need to be interpreted differently. This is because active and passive microwave sensors rely on different physical mechanisms to detect and map snow zones. Active microwave sensors rely more on spatial differences in radar backscatter strength, which are affected by relatively long-term variations of the grain size, density, stratigraphy, and surface roughness of snow pack. In contrast, passive microwave sensors depend on the short-term variations in brightness temperature, which are induced by the changes in the liquid water content of snow pack. Our analysis suggests that the melt snow zone extracted from active SAR imagery does not necessarily coincide with the snow melt extent for the year when the satellite SAR imagery was acquired. Instead, it may indicate an averaged extent of snow melt over many years prior to the image acquisition date. The use of the passive microwave data is able to delineate daily snow melt extent directly corresponding to the acquisition date of the passive microwave data at a much coarser spatial resolution.

The snow zone boundaries derived from the 1997 winter Radarsat SAR image mosaic have a high positional accuracy and contain unprecedented details about spatial extent and geometric shape of different snow zones. These high-resolution snow zone boundaries will be useful for scientific investigations of the Antarctic snow surface. While the whole sequence of snow zones has been identified for the Greenland ice sheet, the superimposed bare ice zone is absent in Antarctica due to its high latitude and less intensive surface melting. Blue ice patches were delimited in both percolation zones and dry snow zones. The blue ice areas are composed of solid bluish ice. Bare blue ice fields are renowned as meteorite collection sites and ideal inland runway sites [4]. There is no net annual snow accumulation in blue ice areas. The formation of the blue ice areas is due to sublimation and katabatic wind scouring, in contrast to the superimposed bare ice zone in Benson's model that is formed by strong melting and is located at the outer edge of the wet snow zone.

Surface melting in the Antarctic continent is relatively sparse and short-lived. The dry snow zone dominates the Antarctic continent, and the melt snow zone accounts for only 10.2 % of its snow surface. Passive microwave data can only provide a coarse discrimination of the melt snow zone from the dry snow zone, while the radar imagery acquired from active SAR sensors can support further differentiation between the percolation zone and wet snow zone within the melt snow zone.

ACKNOWLEDGMENT

This work was supported by the NASA grant NAG5-10112 and the NSF grant No. 0126149. The authors want to thank the National Snow and Ice Data Center (NSIDC) in Boulder, Colorado for providing the SSM/I EASE-Grid brightness-temperature data for this research project.

REFERENCES

[1] H. Liu, L. Wang and K. Jezek, "Wavelet-transform based edge detection approach to derivation of snowmelt onset, end and duration from satellite passive microwave measurements," International Journal of Remote Sensing, (in press) 2005.

[2] K.C. Jezek, "Radarsat-1 Antarctic Mapping Project: change detection and surface velocity campaign," Annals of Glaciology, 34, pp. 263-268, 2002.

[3] C.S. Benson, "Stratigraphic studies in the snow and firn of the Greenland ice sheet," SIPRE Res. Rep. 70, 1962.

[4] [1] R.S. Williams, T. K. Meunier, and J. G. Ferrigno, "Blue ice, meteorites, and satellite imagery in Antarctica," Polar Record, 22 (134), pp. 493-496, 1983.

[5] H. Liu and K.C. Jezek, "A complete high-resolution coastline of Antarctica extracted from orthorectified Radarsat SAR imagery," Photogrammetric Engineering & Remote Sensing, 70(5), pp. 605-616, 2004.

[6] M. B. Giovinetto and H. J. Zwally, "Spatial distribution of net surface accumulation on Antarctic ice sheet," Annals of Glaciology, 31, pp. 171-178, 2000.